

## Constitutive and ligand-induced nuclear localization of oxytocin receptor

Conan G. Kinsey <sup>a, d</sup>, Gianni Bussolati <sup>b \*</sup>, Martino Bosco <sup>b</sup>, Tadashi Kimura <sup>c</sup>, Marie C. Pizzorno <sup>a</sup>, Mitchell I. Chernin <sup>a</sup>, Paola Cassoni <sup>b</sup>, Josef F. Novak <sup>a</sup>

<sup>a</sup>Department of Biology, Bucknell University, Lewisburg, PA, USA

<sup>b</sup>Department of Biomedical Sciences and Oncology, University of Torino, Torino, Italy

<sup>c</sup>Department of Obstetrics and Gynecology, Osaka University Graduate School of Medicine, Suita, Osaka, Japan

<sup>d</sup>Present address: University of Rochester Medical School, Rochester, NY, USA

Received: November 7, 2006; Accepted: December 27, 2006

### Abstract

Oxytocin receptor (OTR) is a membrane protein known to mediate oxytocin (OT) effects, in both normal and neoplastic cells. We report here that human osteosarcoma (U2OS, MG63, OS15 and SaOS2), breast cancer (MCF7), and primary human fibroblastic cells (HFF) all exhibit OTR not only on the cell membrane, but also in the various nuclear compartments including the nucleolus. Both an OTR-GFP fusion protein and the native OTR appear to be localized to the nucleus as detected by transfection and/or confocal immunofluorescence, respectively. Treatment with oxytocin causes internalization of OTR and the resulting vesicles accumulate in the vicinity of the nucleus and some of the perinuclear OTR enters the nucleus. Western blots indicate that OTR in the nucleus and on the plasma membrane are likely to be the same biochemical and immunological entities. It appears that OTR is first visible in the nucleoli and subsequently disperses within the nucleus into 4–20 spots while some of the OTR diffuses throughout the nucleoplasm. The behaviour and kinetics of OTR-GFP and OTR are different, indicating interference by GFP in both OTR entrance into the nucleus and subsequent relocalization of OTR within the nucleus. There are important differences among the tested cells, such as the requirement of a ligand for transfer of OTR in nuclei. A constitutive internalization of OTR was found only in osteosarcoma cells, while the nuclear localization in all other tested cells was dependent on ligand binding. The amount of OTR-positive material within and in the vicinity of the nucleus increased following a treatment with oxytocin in both constitutive and ligand-dependent type of cells. The evidence of OTR compartmentalization at the cell nucleus (either ligand-dependent or constitutive) in different cell types suggests still unknown biological functions of this protein or its ligand and adds this G-protein-coupled receptor to other heptahelical receptors displaying this atypical and unexpected nuclear localization.

**Keywords:** oxytocin receptor • nucleocytoplasmic transport • nuclear inclusions • nucleolus

### Introduction

The study of the oxytocin/oxytocin receptor (OT/OTR) system increasingly focuses on tissues

other than the classical oxytocin peripheral targets, such as breast and uterus, which are mainly involved in reproductive functions [1, 2]. OTR was recently described in a variety of normal tissues (reviewed in [3]) and primary cell cultures including – among others – those derived from prostate [4, 5], endothelium

\*Correspondence to: Gianni BUSSOLATI  
Department of Biomedical Science and Human Oncology,  
University of Torino, Via Santena 7, 10126 Turin, Italy.  
E-mail: gianni.bussolati@unito.it

[6], muscle [7], and bone [8]. OTR is also expressed in a variety of neoplastic tissues [1, 4, 9, 10] and established neoplastic cell lines [11–13] in which it mediates various OT effects.

OTR is a seven-membrane spanning receptor that signals via trimeric G-protein complexes to a phosphoinositide-linked pathway [14], although it also appears to be coupled to other signal transduction mechanisms including cAMP/PKA [15,16], ERK2 [17] and mitogen-activated protein kinase (MAP) [17, 18]. Both the signaling pathways and the biological effects of the OT/OTR system seem to depend on species, type of tissue, physiological versus neoplastic state and receptor location within the cell membrane [19]. The presence of OTR in a variety of tissues and the different effects determined following OT/OTR binding suggests the possibility that the OT/OTR system may have wider biological activities than previously thought.

Heptahelical transmembrane G-protein coupled receptors (GPCR) – to which OTR belongs – are cell surface proteins involved in the transduction of extracellular signals to the cell interior. Upon activation by extracellular ligand binding, the receptor associates to heterotrimeric G-proteins, which interact with downstream effectors (such as enzymes or channels) to generate cellular signals in the form of second messengers or variations in ion concentration. According to the classical view, these events are thought to occur at the plasma membrane and in the sub-plasma membrane cytosolic compartment following receptor endocytosis. The regulation of gene expression by GPCRs is commonly thought to rely on signal transduction from cytosolic mitogen activated kinases (MAPK) to transcription factors and to their subsequent transport in the nucleus [20]. However, recent evidence suggests nuclear translocation of several GPCRs upon ligand binding from an extracellular source or by endogenously produced and not secreted ligand [21]. The activation-induced nuclear localization of GPCRs suggests the presence of a novel mechanism of transcriptional regulation relying on signals directly generated in the nucleus by GPCR-heterotrimeric G-protein-effector complexes [22].

Here we report that OTR localizes to several compartments within nuclei of cells derived from neoplastic breast epithelium, normal connective tissue and osteosarcomas. In addition, we found that translocation of OTR into the nuclei of some types of cells is constitutive whereas in others it depends on ligand exposure.

## Material and methods

### Construction of oxytocin receptor expression plasmids

The OTR cDNA was amplified from a plasmid containing the OTR cDNA [23, 24] using the forward primer 5'-ATG-GAGGGCGCTCGCA-3' and the reverse primer 5'-CGCCGTGGATGGCTGGGA-3' in a PCR reaction. The amplified OTR cDNA (1167 bp without the stop codon) was ligated into the pCRII T/A cloning vector (Invitrogen, Carlsbad, CA) using T4 DNA ligase. The ligation reaction was used to transform TOP10F' One Shot™ cells (Invitrogen). Colonies were selected by ampicillin resistance and screened with Xgal/IPTG. Isolated plasmid DNA was digested with *EcoRI* to confirm those with the desired insert. The plasmids were also digested using *SacI* and *SacII* resulting in a 1116 bp fragment from the sense inserts and a 141 bp fragment from the antisense inserts. Plasmids were produced in *E. coli* and purified by CsCl density centrifugation. Sequencing was performed at the Maine Sequencing Facility (Orono, ME). The fidelity of the sequences was compared with the known sequence (GenBank accession #NM\_000916).

The pCRII-OTR plasmids were digested with *XhoI* and *BamHI* and gel purified by electrophoresis on a 1% agarose/ethidium bromide gel. The bands at 1200 bp were excised from the gel and extracted with ethidium bromide Minus Elution Columns™ (Sigma). The resulting DNA was ethanol precipitated, dried under vacuum and resuspended in ddH<sub>2</sub>O. pEGFP-C1 and pEGFP-N3 vectors (Clontech) were digested with *XhoI* and *BamHI*, separated on a 1.0% agarose gel and extracted as above. Ligation reactions were prepared containing the OTR cDNA and pEGFP-C1 or pEGFP-N3 using T4 DNA ligase. The construction of the pEGFP-OTR plasmids was done in a manner to (i) minimize the number of amino acids between the OTR and GFP, (ii) to assure that both the OTR and GFP sequences were in sense orientation and (iii) that the entire sense sequence of the fusion protein was in frame. The ligation reactions were used to transform chemically competent TOP10F' One Shot' cells (Invitrogen) and the colonies were selected on kanamycin-containing media. The resulting plasmid DNA was digested with *BamHI* and *BglII* and electrophoresed on a 1.0% agarose gel with ethidium bromide. Colonies containing the insert were selected and grown in 500 ml liquid LB cultures containing 30 µg/ml kanamycin. The plasmids were extracted using an alkaline lysis procedure and purified twice by CsCl density centrifugation. The plasmid inserts were sequenced at the University of Maine sequencing facility.

## Cell culture, reagents and anti-OTR antibodies

The human osteosarcoma cell lines, U2OS, SaOS2, MG63 and human breast carcinoma MCF7, were purchased from the American Type Culture Collection (Rockville, MD). OS-9 and OS-15 human osteosarcoma cells were a gift of Dr. Nicola Baldini (Istituti Ortopedici Rizzoli, Bologna, Italy). The primary human foreskin fibroblasts (HFF) cells were a gift of Dr. T. Shenk, Princeton University. The U2OS, MG63 and HFF cell lines were cultured in DMEM/F12 containing 10% heat-inactivated fetal bovine serum (HI-FBS; US Bio-Technologies Inc., Parkerford, PA), 1000 U/ml of penicillin, and 100 µg/ml streptomycin (P/S; GIBCO BRL, Rockville, MD). The MCF7, OS-9, OS-15 and SaOS2 lines were cultured in Iscove's media containing 10% HI-FBS and P/S. When required, the cells were also cultured in VP-SFM serum-free media (Gibco BRL) containing 100 U/ml penicillin, and 100 µg/ml streptomycin. All cells were kept at 37°C in a 5% CO<sub>2</sub> atmosphere.

In order to better assess the specificity and reproducibility of the target identification, three different anti-OTR antibodies were used for IF and western blotting: one monoclonal anti-OTR antibody, 1F3, produced at the University of Torino, whose specificity was assessed by enzyme-linked immuno-adsorbent and immunoblot tests as previously described in detail [1]; two commercial polyclonal antibodies respectively directed towards the N- and the C-terminal of OTR (Research Diagnostic Inc., Flanders, NJ).

## Transfection of cells with the OTR-GFP construct

The cells used for transfections were seeded onto 12 mm diameter round coverslips in 24 well plates and grown to 40–50% confluency over a minimum of 24 hr. The cells were washed twice with sterile saline and incubated with 200 µl of serum-free RPMI media containing 1 µl of lipofectin (Gibco BRL) and 1 µg of plasmid (pEGFP-N3-OTR and pEGFP-C1-OTR) per transfection. The pEGFP-N3 and pEGFP-C1 plasmids were used in control transfections. The cells were incubated at 37°C for 24 hr, overlaid with fresh media, and incubated for another 48 hr before fixation with cold 100% methanol.

## Internalization of surface-bound oxytocin

Two different approaches were employed for studies of surface-bound radioligand: (1) to measure the levels of surface-bound oxytocin by means of an acid-wash, the cells were plated in 24-well plates and grown to confluency. One-day postconfluency, the media were aspirated, replaced with serum-free VP-SFM media (Gibco) and the

cells were cooled to 4 °C for 10 min. The VP-SFM media was removed and replaced with 200 µl of <sup>125</sup>I-OT (new England Nuclear, Boston)/10<sup>-8</sup> M OT in VP-SFM. All control wells received 200 µl of <sup>125</sup>I-OT/10<sup>-5</sup> M OT mixture. The cultures were incubated for 4 hr at 4 °C and transferred into a 37 °C, 5% CO<sub>2</sub> environment for indicated time periods: 0, 5, 10, 20, 30 and 60 min. At the end of the 37°C incubation period the cells were quickly washed 2× with ice-cold PBS and 250 µl of acid wash (0.2 N acetic acid in 150 mM NaCl, pH 2.5) was added followed by incubation at 4°C for 5 min. Finally, the cell layer was dissolved in 0.5 M NaOH at 37°C (10 min). Both acid wash and NaOH-digested fractions were counted in a gamma counter. The final data were corrected for non-specific binding. (2) Flow cytometric analysis of OTR internalization was conducted with subconfluent U2OS osteosarcoma cells incubated with 1 µM OT for 2 hrs at 4°C. The control cells were kept at 4°C for an additional 30 min, whereas the test cells were moved to 37°C for the same time period. Both control and experimental cell samples were incubated with 1 µg 1F3 MAb [1] at 4°C for 60 min. The cells were washed 3× with cold PBS and incubated with a secondary antibody, goat anti-mouse IgM-FITC (Sigma) diluted 1:40 for 45 min at 4°C. Finally, the cells were harvested using a cell scraper and resuspended to a density of 500,000 cells/ml and the intensity of the cell surface-bound fluorescence was recorded by scoring at least 10,000 cells/sample. The data were corrected for background fluorescence intensity that was determined after incubating the cells with the goat anti-mouse IgM reagent alone.

## Nuclei isolation

Cells grown to confluency in 10 cm dishes were washed three times with PBS, trypsinized and collected by centrifugation (400 × *g*). To obtain a pure nuclei preparation (procedure 1) the cells were resuspended in 500 µl of hypotonic buffer (10 mM Tris, 5 mM KCl, 1 mM DTT, 0.15 mM spermine, 0.5 mM spermidine, 2 mM EDTA, 10% glycerol and pH 8.0) and transferred into a microcentrifuge tube. The cell suspension was incubated on ice for 1 min before addition of 15 µl of 10% Triton-X. The suspension was dounced 25 times and incubated on ice for additional 3 min and layered onto 1.0 ml of cushion buffer (10 mM Tris, 5 mM KCl, 1 mM DTT, 0.15 mM spermine, 0.5 mM spermidine, 0.2 M sucrose, 2 mM EDTA and 10% glycerol and pH 8.0) and centrifuged at 10,000 rpm for 10 min. The supernatant was removed, nuclei resuspended in hypotonic/Triton X buffer, passed through a 22-gauge needle [25], and pelleted through the sucrose cushion. Sedimented nuclei were resuspended in 250 µl of Locke's solution for ligand saturation binding studies, immunofluorescence,

and protein analyses, respectively. To obtain a crude nuclear pellet (procedure 2) the straining through the needle and the second sucrose cushion centrifugation were omitted. Protein extracts of pure and crude nuclei were obtained by dissolving nuclei in protein sample buffer prior to electrophoresis.

## Fluorescent immunocytochemistry

Cells were seeded onto 12 mm diameter round coverslips in 24-well plates and grown to 70% confluency. The coverslips were treated with OT ( $10^{-7}$  M) in complete cell culture media. Following OT or control treatment, the cell medium was removed and the coverslips were washed three times with PBS and fixed with 0.5 ml of ice-cold methanol for 10 min. The methanol was removed, the coverslips were dipped into cold acetone for 5 sec and placed back into the wells and rehydrated with PBS for 10 min at 37°C. The PBS was removed and 200  $\mu$ l of 1% BSA was placed on the coverslips and incubated for 1 hr at 37°C to block non-specific binding. The 1% BSA solution was removed, 30  $\mu$ l of anti-OTR monoclonal antibody [1] in a 1:1 dilution with a solution of 1% BSA and 50 ng/ml of RNase A was placed onto the coverslips, and incubated for 4 hr at 37°C. The antibody solution was removed and the cells were washed five times for 5 min with PBS. A solution of fluorescein isothiocyanate-conjugated antimouse IgG antibody (Sigma) diluted 1:200 in 1% BSA and containing 10  $\mu$ g of propidium iodide was added to the coverslips and incubated for 1 hr. The coverslips were washed five times for 5 min and mounted on glass slides using Vectashield mounting media (Vector Laboratories, Inc., Burlingame, CA). The cells were observed using confocal and differential interference contrast (DIC) microscopy. In selected experiments, the nuclear membrane was stained using a primary polyclonal goat anti-lamin B antibody (SC-6217; Santa Cruz, CA, USA), diluted 1:5 in phosphate-buffered saline (PBS) containing 5% bovine serum albumin (BSA). The secondary serum was a fluorescein isothiocyanate-conjugated rabbit anti-goat antibody (Sigma Aldrich, Munich, Germany), diluted 1:200 in PBS containing 5% BSA

## Whole cell protein extraction

Cells were grown to confluency in 10 cm dishes. The media were discarded and the dishes were washed three times with PBS. Cell lysis solution (20 mM MOPS, 0.15 M NaCl, 1% NP-40, 1% sodium deoxycholate, 1 mM EDTA, and 1% SDS; pH 7.4) was added at a ratio of approximately 1 ml per  $10^7$  cells but no less than 0.8 ml per 10 cm dish. The cells were scrapped into a 1.5 ml microcentrifuge tube, vortexed, maintained on ice for 30 min and stored at  $-80^{\circ}\text{C}$ .

## Western blotting of the OTR

Whole cell extracts and nuclear extracts were separated by SDS-PAGE in a 10% polyacrylamide Tris-glycine-SDS gel. The proteins were transferred onto nitrocellulose membranes. The blot was blocked using 10% dry milk in Tris buffered saline containing 0.05% Tween-20 (TBST) for 1 hr with agitation. The blot was washed five times for 5 min with TBST and then exposed to C-terminal specific and N-terminal specific anti-OTR polyclonal antibodies (1:200; Research Diagnostics, Inc., Flanders, NJ) in 1% dry milk/TBST overnight at 4°C. The blot was washed five times for 5 min with TBST and exposed to peroxidase conjugated anti-goat IgG antibody (Sigma) diluted 1:5000 in 1% dry milk/TBST for 30 min at room temperature. ECL<sup>TM</sup> chemiluminescent detection system (Amersham Life Sciences, Piscataway, NJ) was used for visualization of antibody positive bands and blots were exposed to Hyperfilm<sup>TM</sup> for 5 min. For densitometric quantification, the film was scanned using a Molecular Dynamics computing densitometer, model 300A.

## Results

### Internalization of cell-surface OTR

U2OS osteosarcoma cells were equilibrated with  $10^{-9}$  M extracellular  $^{125}\text{I}$ -OT at 4°C and the loss of cell surface label was followed in a time-dependent manner in the presence or absence of excess OT. By the acid wash technique, it was established that approximately 85% of total cell surface-localized  $^{125}\text{I}$ -OT is internalized within the first 20 min after ligand addition (Fig. 1A). These data suggest that the internalization of cell-surface bound radioactive OT begins immediately following the receptor ligand binding.

The fate of cell surface OTR protein was also determined by means of flow cytometry of cells labeled with OTR-specific antibodies conjugated to FITC [26]. The incubation of cells with 1  $\mu$ M OT at 37°C was followed by a significant decrease (approximately 50%) of the number of cell surface OTR receptors (Fig. 1B). In summary, the results shown in Fig. 1A and 1B suggest that either the cell surface-bound  $^{125}\text{I}$ -OT becomes progressively resilient to recovery by acid-wash or the OTR, following its occupancy by a ligand, is no longer recognizable on the surface of the cell membrane by specific antibodies. These results support the conclusion that cells internalize both the receptor and its ligand.

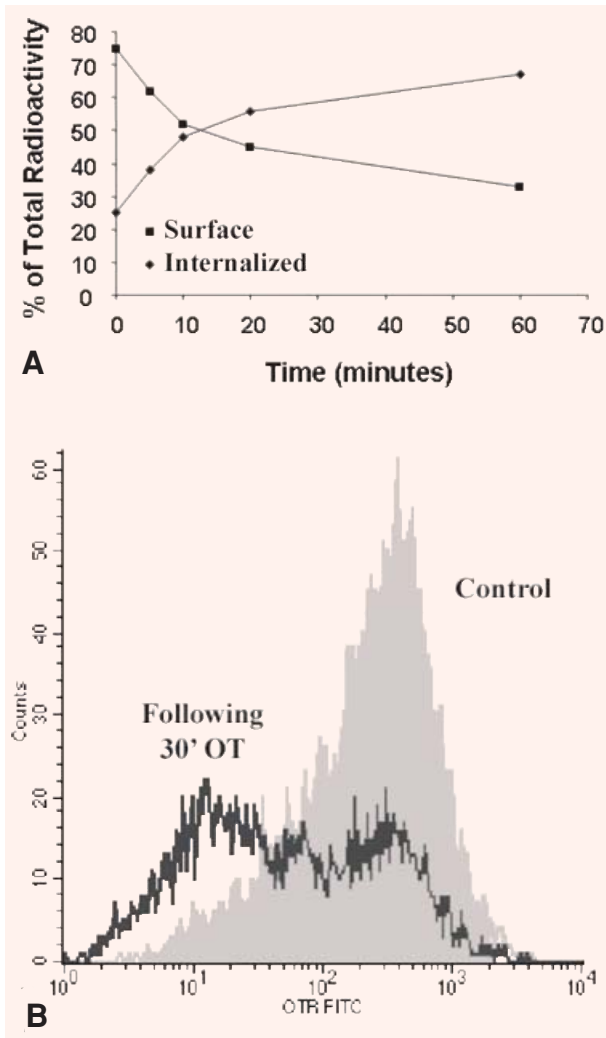


**Fig. 1** Cell-surface ligand is internalized by OT (oxytocin)-treated cells. **(A)** Acid-wash method using <sup>125</sup>I-oxytocin. For OT internalization by the acid-wash technique, confluent cultures of U2OS cells were washed and cooled to 4°C before adding <sup>125</sup>I-OT and cold OT to a final concentration of 10<sup>-9</sup> and 10<sup>-5</sup> M, respectively. The binding was equilibrated at 4°C for 4 hrs. At the end of the binding period, the cells were transferred to 37°C for the indicated time periods. The cells were washed, treated with acid wash and finally dissolved (see 'Methods'). Both acid wash (representing the <sup>125</sup>I-oxytocin fraction bound at the surface) and the cell digest (representing the <sup>125</sup>I-oxytocin fraction internalized) were collected and their radioactivity determined. Lines are the mean of two different experiments. Standard deviation were less than 10%. **(B)** Flow cytometry method using a specific antibody to human OTR. Flow cytometry of OT internalization was performed using cells equilibrated with 10<sup>-9</sup> M OT at 4°C. The hormone-equilibrated cells were then incubated for additional 30 min either at 4 or 37°C. The cell surface OTR was labeled sequentially with 1F3 MAb and FITC-secondary antibody. The cells were scrapped and analysed by means of flow cytometry.

## Localization of OTR-GFP fusion protein

Two OTR-GFP plasmids were constructed, one with the GFP at the amino terminus and one with GFP at the carboxyl terminus. Transfection of these plasmids into cells showed that the N-terminal fusion failed to express functional membrane-bound OTR (results not shown), a result noted by others [27]. Since only the C-terminal fusion, here designated as OTR-GFP, was stably expressed as a membrane bound form, all further studies were carried out with this expression vector.

The functionality of the OTR-GFP fusion protein was ascertained by cytological relocation of the expressed fusion protein following treatment of cells with OT. Midsection confocal microscopy images of transfected MCF-7 cells are shown in Fig. 2. Prior to the

treatment with OT, the OTR-GFP fusion protein appears equally distributed between cell surface and cytoplasm with essentially no fluorescence in the nucleus (Fig. 2A). For translocation of OTR-GFP from cell membrane/cytoplasm to nuclei, the MCF-7 cells required treatment with exogenous OT (10<sup>-7</sup> M). Fifteen minutes after treatment with OT (Fig. 2B) nearly all of the OTR-GFP was sequestered into cytoplasmic vesicles, which appeared equally distributed throughout the cytoplasm. Continuous 24-hrs treatment with OT (Fig. 2C) resulted in concentration of the granular fluorescence around the nucleus with some accumulation of GFP-generated fluorescence within the nucleus itself. After 48 hrs of continuous OT treatment, the MCF7 cells exhibited large OTR-containing vesicles within the cytoplasm (Fig. 2D), some accumulation around the nucleus and a distinct

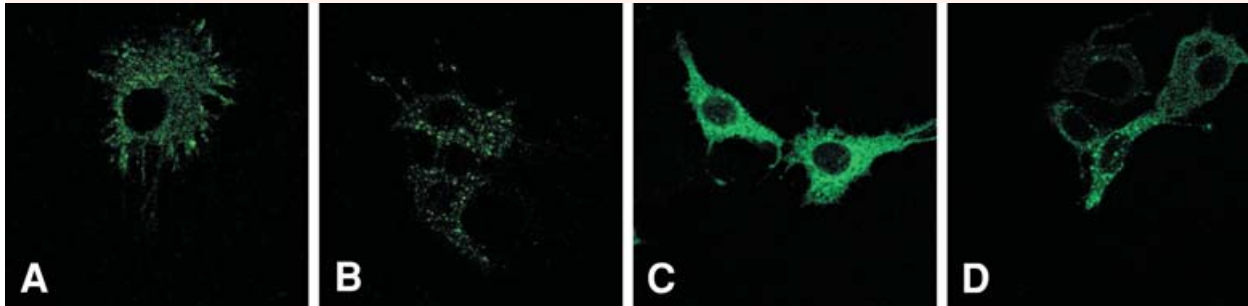


**Fig. 2** Midsection confocal microscopy of OTR-GFP in pEGFP-N3-OTR-transfected MCF7 cells before (A) and after (B–D) OT treatment. Cells in images (B–D) were treated with OT ( $10^{-7}$  M) for 15 min, 24 and 48 hrs, respectively. While the control nuclei (A) are essentially free of the GFP-mediated fluorescence, their intensity increased with length of OT treatment.

localization of fluorescence within the nuclei of some but not of all the cells. In control experiments transfected with GFP plasmid alone, the fluorescence became evenly distributed within the cytoplasm and nucleus soon after the expression of the GFP. The process of GFP distribution was not affected by a treatment with OT (results not shown).

In contrast to MCF-7 cells, the OTR-GFP protein in U2OS osteosarcoma cells exhibited strong staining within the nucleus even in the absence of OT treatment (Fig. 3A). OT treatment of U2OS cells resulted in increased vesiculation of OTR-GFP protein. The vesicles surrounded the nucleus followed by a time-dependent increase of the amount in fluorescence within the nucleus (Fig. 3B–E). In other experiments we found a number of other osteosarcoma cell lines (MG-63, SaOS2 and OS-15) localize OTR-GFP into the nucleus with or without OT treatment (see below). The time-point of initial localization of OTR-GFP into the nucleus in osteosarcoma cells is difficult to assess as the expression and translocation of the fusion protein overlaps with the transfection procedure itself. Regardless, transfection experiments revealed a difference between MCF7 breast carcinoma and a number of osteosarcoma cell lines in terms of OTR-GFP sub-cellular localization and responses to the treatment with a ligand. It is also possible that the slow kinetics of GFP-OTR nuclear localization in MCF-7 cells was due to a cell-specific interference by GFP in the translocation of OTR-GFP. In order to resolve this possibility, the localization of endogenous OTR within cells was examined using a monoclonal antibody specific for the OTR.

### OT-dependent and independent distribution of endogenous OTR

Immunofluorescence avoids problems associated with expression of the OTR-GFP gene, particularly the presence of the overexpressed protein in the cell, time required for expression of the fusion protein, and possible interference of GFP with either the translocation of OTR across the nuclear pore or the interaction of OTR with karyophylic proteins. Similarly to OTR-GFP experiments, immunofluorescence studies of endogenous OTR in MCF7 cells show that both internalization and nuclear localization of the OTR is strictly dependent on treatment of cells with ligand (Fig. 4). In MCF7 cells, the OT-dependent nucleoplasmic transport of OTR can be observed within minutes following the addition of ligand. However, only a minor portion of total cytoplasmic OTR enters the nucleus, while most of the label accumulates in the perinuclear region. Once transported into the nucleus, the OTR remained within the nucleus regardless of the extracellular presence of OT for at least several hours (results not shown). Conversely, the endogenous OTR localize into the nuclei of bone cancer derived U2OS cells (Fig. 5A–C) and SaOS2 cells (Fig. 5D–E) regardless of OT treatment. Nuclear transport of OTR in normal human fibroblasts (HFF) cells is only partially dependent on exogenous OT; however, its nuclear localization is greatly enhanced by OT treatment (Fig. 6).

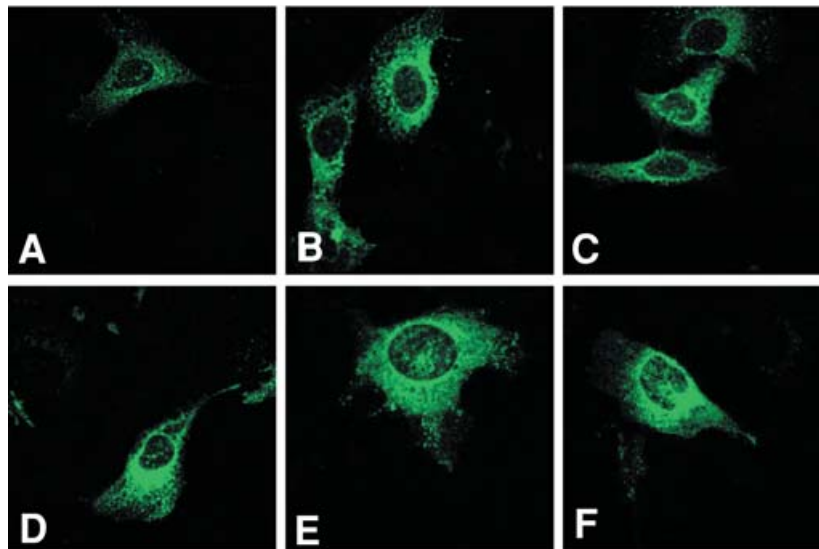


**Fig. 3** Constitutive and time-dependent translocation of OTR-GFP into the nuclei of U2OS cells. Image **A** represents midsection confocal microscopy of the untreated cells, 2 days post-transfection with pEGFP-N3-OTR (time 0). Cells in images **B** through **F** were all treated with OT ( $10^{-7}$  M) for 6, 24, 48, 72 and 96 hrs, respectively.

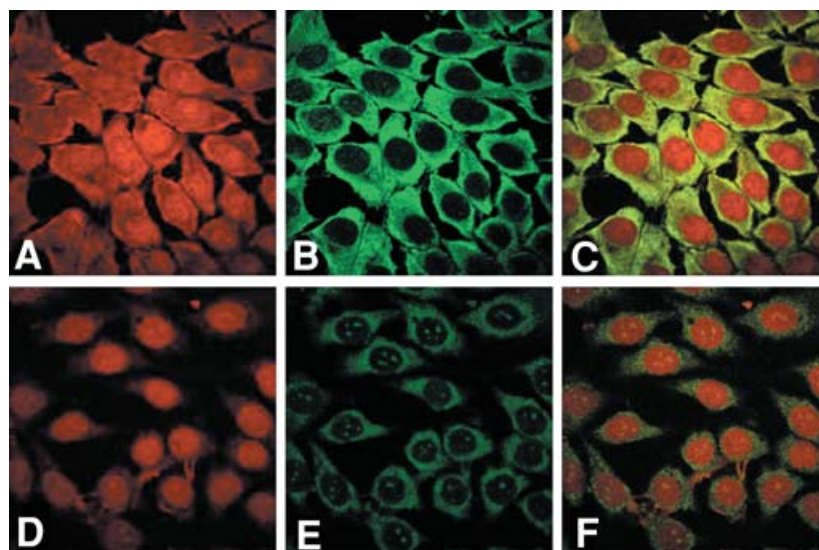


**Fig. 4** Midsection confocal immunofluorescence microscopy of ligand-dependent nuclear localization of endogenous OTR in MCF-7 cells. Cells in images (**A–C**) represent OT-untreated controls. Cells in images (**D–F**) were treated with OT  $10^{-7}$  M for 15 min. Staining obtained with propidium iodide stain (**A** and **D**) and anti-OTR antibody FITC immunofluorescence (**B** and **E**). **C** and **F** are overlays of **A** and **B**, and **D** and **E**, respectively.

## Properties of intracellular OTR

### Relationship between perinuclear and nuclear OTR

Whole cell protein preparations and nuclear protein extracts of U2OS osteosarcoma cells were prepared and separated on SDS-polyacrylamide gels. Western blots revealed the expected ~59 kD OTR in whole cell extracts as well as nuclear fractions (Fig. 7). Only about 6% of total OTR present in the cell membrane could be seen in the nuclear fraction of HFF cells; however, this amount increased fourfold following treatment with OT (Fig. 8). These results are in keeping with constitutive and ligand-induced accumula-

tion of OTR in the proximity of the nucleus as indicated by fluorescence microscopy. Thus, the 'nuclear fractions' analysed by Western blot could include OTR isolated from the vicinity of the nucleus as well as that localized exclusively within the nucleoplasm.

We set out to directly determine to what extent the material reacting with the OTR-antibody remains associated with isolated nuclei. In order to highlight this perinuclear component, we used an abbreviated nuclear isolation procedure designed to obtain nuclei with an excess of the nuclear-associated cytoplasmic fragments (crude nuclei; procedure 2 in 'Methods'). Nuclear preparations from OT-treated and -untreated MCF7

**Fig. 5** Ligand-independent transport of endogenous OTR into nuclei of U2OS (A–C) and SaOS2 (D and E) osteosarcoma cells. The cells were either untreated (A–D) or treated for 15-min with  $10^{-7}$  M OT (E). Images were obtained by means of midsection confocal microscopy of cells stained with propidium iodide (A), or immuno-fluorescence using a monoclonal OTR antibody and FITC conjugated rabbit antimouse IgG (B–E). C is an overlay of A and B.

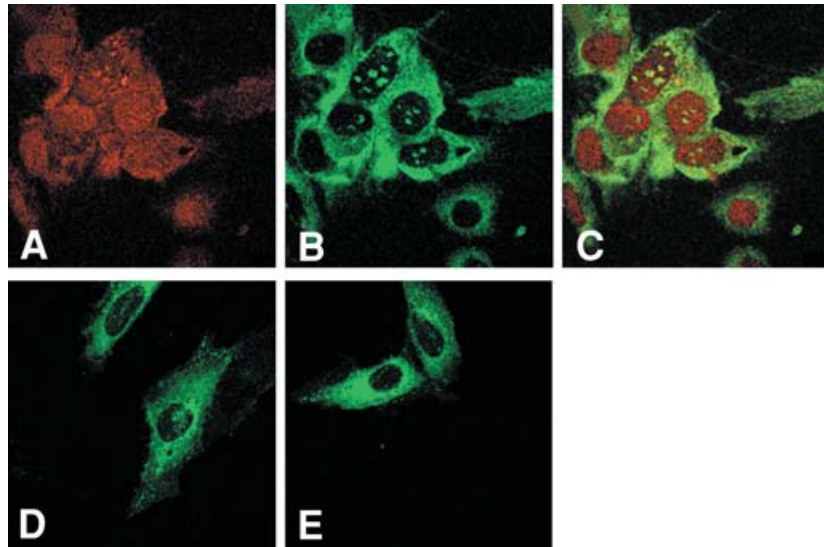
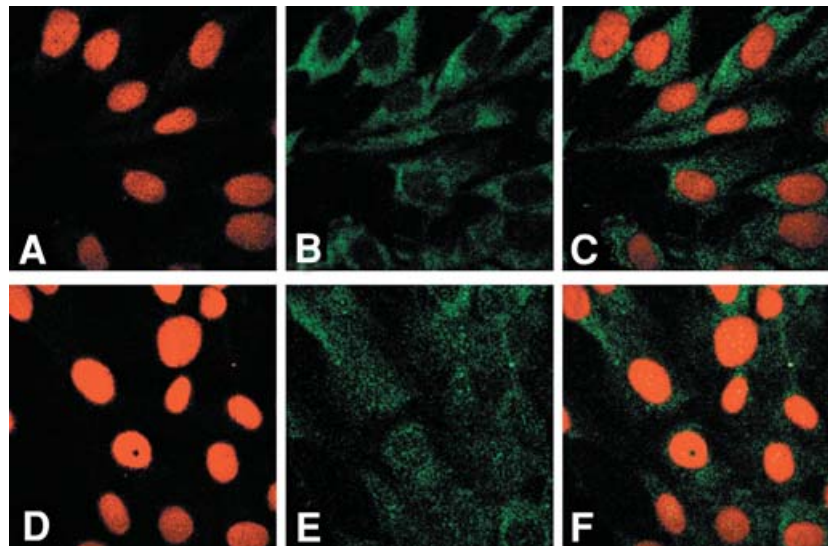


**Fig. 6** Midsection confocal microscopy images of primary human fibroblast (HFF) cells. Images A through C were obtained from control (OT-untreated cultures) while images D through F were from cultures treated with OT at  $10^{-7}$  M for 15 min. Images A and D represent staining with propidium iodide, images B and E are immuno-histochemistry using monoclonal OTR-antibody and FITC conjugated rabbit anti-mouse IgG, and images C and F are overlays of images A and B, and D and E, respectively.



cells were fixed and subjected to immunofluorescence confocal microscopy. The results showed that nuclei of MCF7 cells lack OTR in the absence of OT treatment (Fig. 9). There was, however, a significant increase of OTR within nuclei as well as the perinuclear cytoplasm following OT treatment.

#### **OTR localizes into nucleoli and nucleoplasm**

The OTR localization appears to be in several regions of the nucleoplasm of HFF cells. The retention of both OTR-GFP and native OTR within the nucleus last hours to days (Fig. 3). In nearly all images examined, the OTR (or OTR-GFP) could be

seen in the nuclei of cells as specks (4–20 in number), with ill-defined margins. The large specks are surrounded by smaller antibody-positive dots too numerous to be enumerated (Fig. 10A) and are near the geometrical midline of the nucleus (Fig. 10B); in no instance is the OTR associated with the internal nuclear envelope. The latter is further documented by double-staining the cells for lamin B and OTR (Fig. 11). In some instances, OTR was distinctly localized into at least one of the nucleoli (Fig. 12A–B) as demonstrated by superimposing the DIC and fluorescence images of the same field. It appeared that the nucleoli staining occurred prior to treatment with a



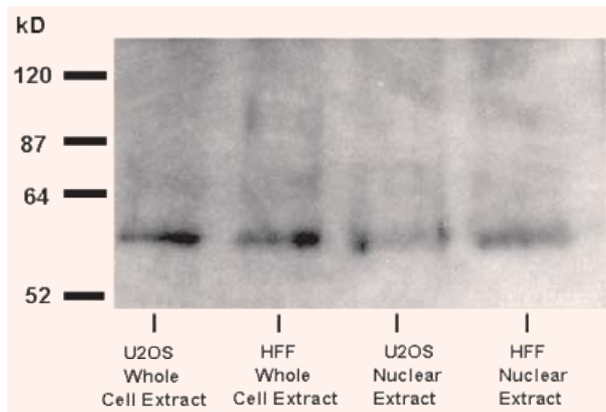


**Fig. 7** Western-blot analysis of OTR in U2OS and HFF cells. The cells were treated with OT  $10^{-7}$  M for 15 min. Following the hormone treatment, the cells were used either for the isolation of total protein (whole cell extract) or for isolation of nuclei. The purified nuclear fraction (procedure 1 in the 'Methods') was then used for isolation of total nuclear protein extract.

ligand (Fig.12C–D). The reason for localization of OTR to some of the nucleoli in some cells, and in certain cases, to all nucleoli of the same cell, is not known.

### Bone cancer cells produce increased levels of OTR

The immunofluorescence observations of a variety of cells indicated quantitative differences in their content of intracellular OTR. The level of OTR antibody-mediated staining was consistently higher in osteosarcoma cells than in any of the other cells studied. We employed Western blotting to estimate the relative amount of OTR produced by various cell lines. When equal amounts of total protein were loaded onto SDS-PAGE gels, subsequent densitometric analysis of Western blots showed that osteosarcoma cells produce  $3.6\times$  as much OTR as HFF cells and  $20\times$  the amount produced by MCF7 breast cancer cells (Fig. 13). It appears, therefore, that the osteosarcoma cells not only exhibit a ligand-independent nuclear translocation mechanism, but also produce increased levels of the OTR in comparison to the non-bone tumours or normal cells examined.

### Discussion

In this study, we report that OTR localizes to different compartments within nuclei derived from neoplastic

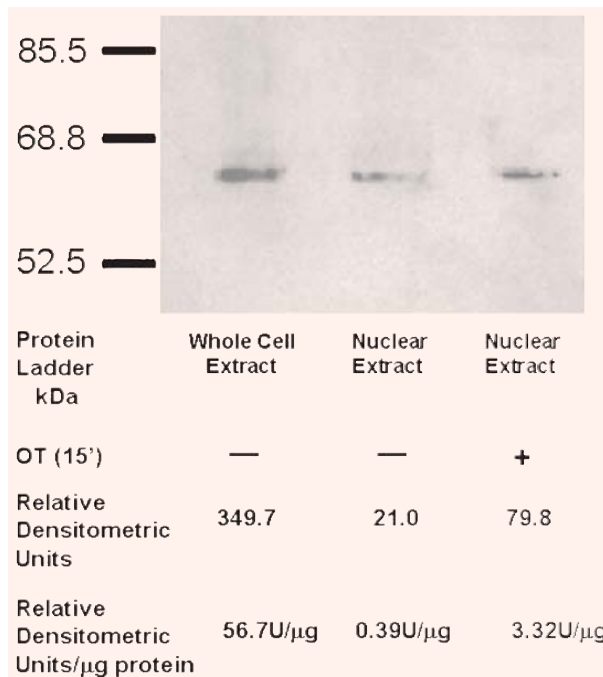
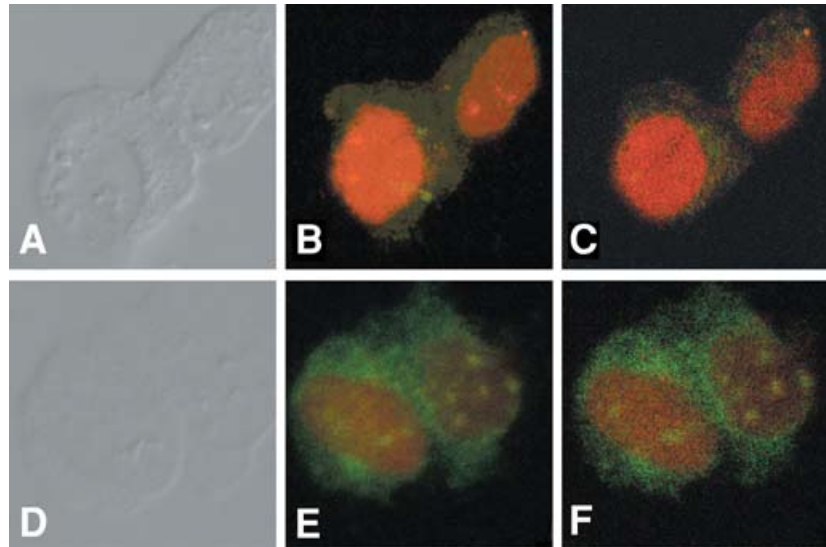


**Fig. 8** Treatment with OT increases translocation of OTR into nuclei of HFF cells. Western-blot indicating the presence of the OTR in nuclear protein fractions (procedure 1, 'Methods') of both control and OT-treated ( $10^{-7}$  M, 15 min) HFF cells. The relative densitometric units (U) per microgram of protein indicate approximately 10 times higher level of OTR in OT-treated cells. The total amount of protein loaded onto the wells is as follows: whole cell extract (60.75  $\mu$ g), nuclear extract (54  $\mu$ g) and nuclear extract from cells treated with OT (24  $\mu$ g).

and normal cells. In addition, we show that translocation of OTR into the nuclei of some types of cells is constitutive while in others it is dependent on treatment with oxytocin. Although the localization of OTR to the nucleus is a novel finding, many other surface receptors, including other GPCR, were previously shown to be located within this organelle [21]. In the past, attempts to locate intranuclear receptors were hindered by uncertainties such as cytoplasmic contamination of isolated nuclei and, most importantly, from the reliance on epifluorescence microscopy that could not conclusively distinguish between nuclear, cytoplasmic and plasma membrane labelling. The advent of confocal microscopy, GFP technology and specific antibodies with localization-enabling tags has allowed unambiguous characterization of several nuclear receptors previously known to occur only

**Fig. 9** Association of OTR with the perinuclear and nuclear fractions of MCF-7 cells. **A–C** depict control cells and **D–F** represent OT-treated ( $10^{-7}$  M for 15 min) cells. **A** and **D** are phase contrast images, **B** through **F** are confocal images of immuno-fluorescence with OTR-Ab, FITC-labeled conjugate and propidium iodide. **B** and **E** are stacked confocal images while **C** and **F** are a single midsection images.



in association with the plasma membrane. The precise localization of GPCR and other surface membrane receptors in the nucleus is not known. However, some nuclear membrane systems derived from the invagination of the outer and/or the inner nuclear envelope or, alternatively, nuclear non-membranous lipophilic domains have been suggested as possible sites for the nuclear localization of integral membranous proteins such as GPCR [28].

In this study, confocal immunofluorescent microscopy of OT-treated cells showed OTR-strongly labelled endoplasmic reticulum associated with the outer nuclear envelope as well as the antibody-positive material within the nucleus. It was observed that the OTR-staining was associated with different parts of the nucleus and assumed several morphological characteristics: (1) several patchy loci scattered within the nucleus; (2) well-defined nuclear dots not dissimilar from those known as PML bodies (ND10) [29]; (3) a clearly delineated nucleolar localization, particularly following transfections with OTR-GFP or before OT treatment in immunofluorescence studies and (4) dispersed small well-delineated spots within the nucleoplasm. It was of interest to experimentally verify ligand-induced accumulation of OTR to the perinuclear and nuclear compartments using isolated nuclei. We sought to confirm the immunofluorescence data by observing physical association of OTR with crude nuclei preparations which accent perinuclear cytoplasmic constituents, and OTR distribution observed *in situ* by immunofluorescence using isolated nuclei. The results of these exper-

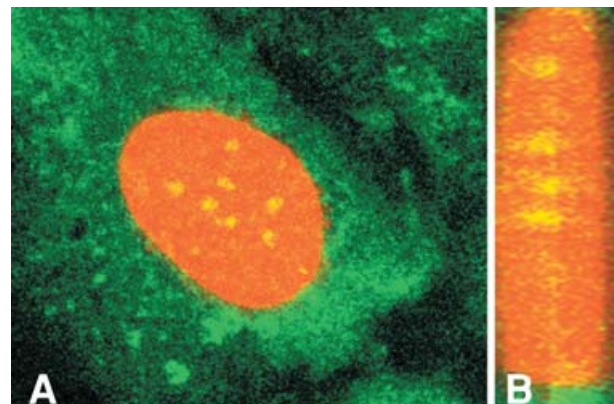


**Fig. 10** Confocal immunofluorescent microscopy showing maximum projection stacked images of a single HFF cell from cultures treated with  $10^{-7}$  M OT for 5 min. Image **A** shows the front view of the cell. **B** shows a segment of the nucleus that was selected for  $90^\circ$  rotation. The resulting image documents distinct localization of OTR along the midline of the nucleus.

iments were indeed similar.

Nuclear OTR was evident in several osteosarcoma cell lines with or without prior treatment with exogenous OT. In contrast, cells other than those of bone neoplastic origin required treatment with OT in order to translocate their OTR into the nuclear compartment. Human foreskin fibroblasts exhibited an intermediary behaviour as some OTR could be detected in nuclei of these cells without OT treatment. Nevertheless, these cells responded with a robust transport of OTR into the nucleus following

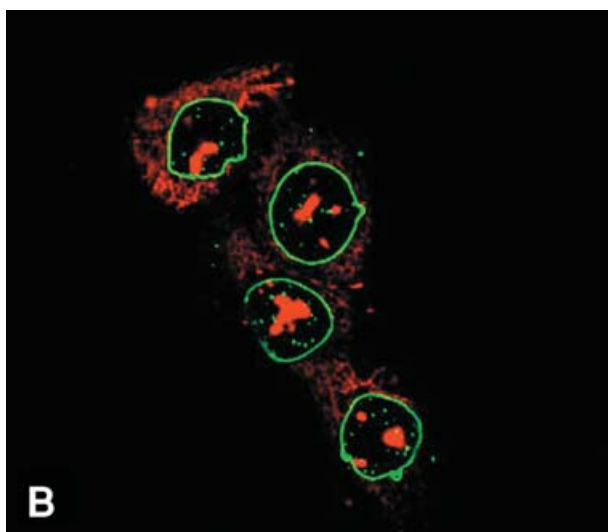
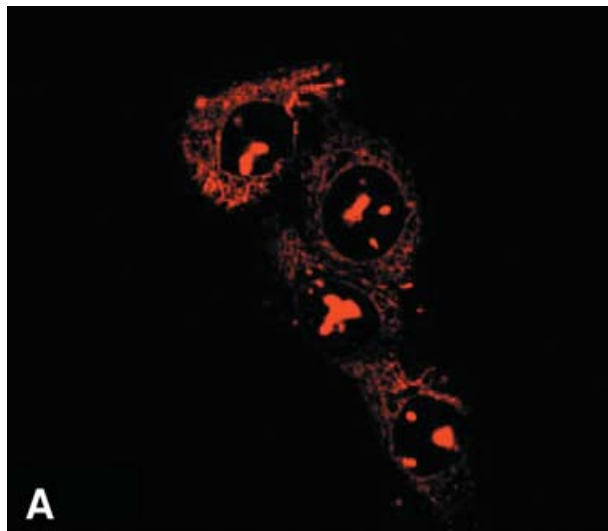


**Fig. 11** Nuclear OTR does not interact with nuclear envelope. U2OS cells grown on coverslips were fixed/permeabilized and double staining was performed using anti-human lamin B (green, **B** and **C**) and with anti-OTR 1F3 (red, **A**, **B**, and **C**) Mab as described in the 'Methods'. The image was obtained by confocal microscopy of a nucleus midsection and shows the lack of association of OTR with the internal nuclear envelope.

OT-treatment. The presence of a ligand-induced nuclear transport of OTR in some cell lines suggest that the nuclear localization of OTR could have some functional role in the cellular response to OT. The fact that in osteosarcoma cells the OTR translocates into the nucleus even in the absence of OT may be caused by constitutive activation of the mechanism involved in the nuclear import of OTR which specifically affect bone-derived neoplastic cells. As a possible interpretation, we could hypothesize the involvement of some bone extra-cellular matrix molecules specifically produced in bone neoplastic cells in promoting the OT-independent OTR translocation into the nucleus. In a previous study from our group, we described the presence of a functional plasminogen

activator system on the surface of bone neoplastic cells promoting the cleavage of the bone matrix protein osteocalcin [12]. Matrikines (extracellular matrix molecules, such as tenascin and its EGFR-like repeats, *i.e.*) [30] have been reported to be possibly involved in the activation of membrane receptors of growth factors (*i.e.* EGFR) favoring the internal trafficking and even their eventual nuclear translocation [30]. Our challenging hypothesis is that, in our experimental model, bone matrix molecules associated with bone neoplastic cells could account for the OT-independent, cell-type specific nuclear translocation of OTR.

To further complicate our scenario, a high aminoacid homology (five out of six) between the high affinity E2 region of OTR and an osteocalcin-derived hexa-

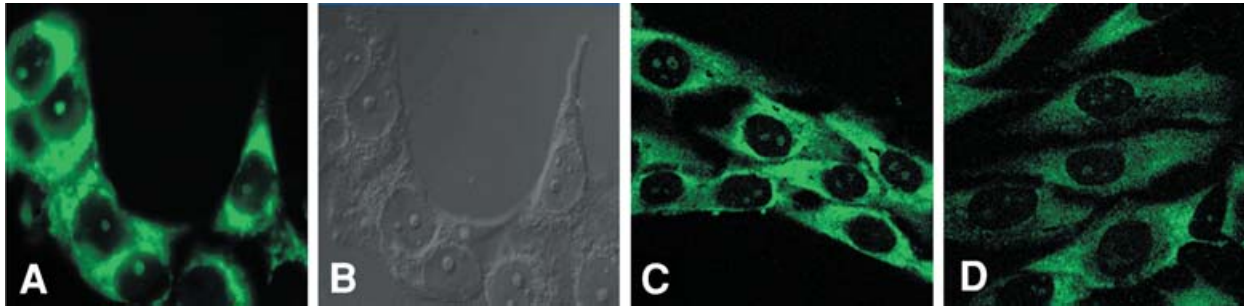


**Fig. 12** Nucleolar localization of OTR in MCF-7 and MG-63 cells. Standard epifluorescent immunocytochemistry (A) and DIC phase contrast microscopy (B) images of the same group of MCF-7 cells show distinct nucleolar localization of OTR. MCF-7 cells were stained with anti-OTR MAb and a FITC-conjugated rabbit anti-mouse IgG (A). Images C and D represent midsection confocal microscopy of MG63 osteosarcoma cells stained with the same antibodies as above. Control cells (C) were not treated with OT, while the cells in image D were treated with  $10^{-7}$  M OT for 15 min.

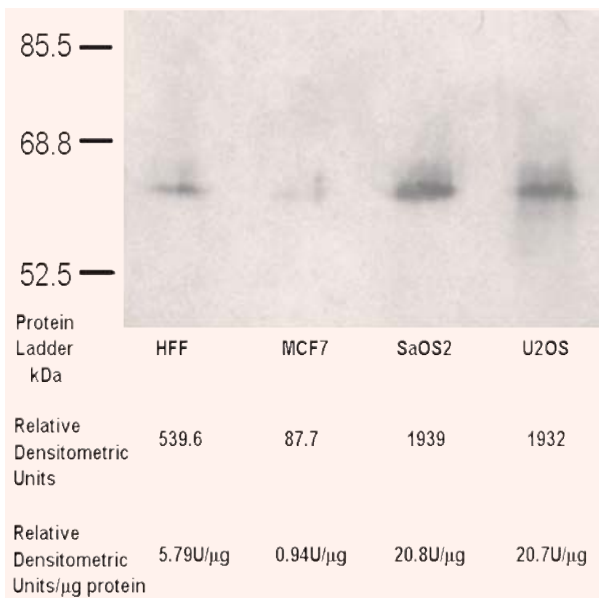


**Fig. 13** Osteosarcoma cells overproduce OTR. Western-blot of OTR present in whole cell protein extracts obtained from HFF, MCF7, SaOS2 and U2OS cells, respectively. The total amount of protein loaded onto gels was adjusted to 93  $\mu$ g per each well. The blots were developed according described methods and subjected to quantitative analysis. The densitometric data indicate (Relative Densitometric Units, U) that both osteosarcoma cell lines tested produce as much as  $3.6\times$  more OTR as HFF cells and  $20\times$  more OTR in comparison to MCF-7 cells.

peptide has been described [12]. It cannot be excluded that such structural similarity could participate in osteosarcoma-cells specific OT-independent nuclear translocation of OTR through an unknown mechanism of receptor activation.

OT causes accumulation of OTR in the perinuclear region in all cells regardless of whether they exhibit constitutive or ligand-dependent OTR nuclear localization. The accumulation of OTR around the outer nuclear membrane may represent a necessary step for nuclear uptake or it may be the result of an independent process. The latter appears to be more likely as high perinuclear levels of OTR do not necessarily translate into higher nuclear uptake.

The transport of a membrane receptor to the nucleus could be attributed to the presence of a peptide sequence called the nuclear localization sequence (NLS). Putative simple and bipartite NLSs are located within the cytoplasmic but not the extracellular segments of the OTR and include the following three clusters of positively charged amino acids with a strong homology to known NLS sequences [31]: RTTRQKHSR (1<sup>st</sup> intracellular loop [i.l.], aa 65-73, RSLRRRTDR (2<sup>nd</sup> i.l., aa 146-154) and KGRR-7aa-KK (C-terminus, aa 353-365). The RSLRRRTDR sequence also bears a similarity to the HIV-1 Rev nucleolar localization sequence (NoLS) described by Cullen *et al.* [32] and to similar sequences compiled by Thebault *et al.* [33]. We have observed distinct nucleolar localization in some experiments, while in others the OTR exists as spots dispersed throughout the nucleoplasm. This raises the possibility of (i) single import pathway into the nucleolus followed by dispersion of the OTR into nucleoplasm or (ii) dual import mechanisms (NLS and NoLS) for the OTR. Alternative mechanism for the nuclear import of OTR and other GPCRs include interaction with carrier proteins containing a NLS [34].

Translation from alternative start codons represents another mechanism that may determine the destination of the protein product. Fibroblast growth factor that is translated from the first AUG codon is cytoplasmic while isoforms that initiate from upstream in-frame CUG codons translocate into the nucleus [35, 36]. Similarly, PTHrP expressed from an AUG start codon is directed to the cell membrane, whereas peptides expressed from alternative CUG and GUG start codons are redirected to other sites within the cell, including the nucleus [37]. Kimura *et al.* [23] showed expression of 4.4, 3.6 kb, and possibly other minor OTR mRNA species from mammary gland and term myometrium. Multiple OTR mRNA species were also identified using various 3' UTR-derived probes [38]. The plausible existence of destination-determining signals within the OTR mRNA is an attractive hypothesis because it could impart translocation of different OTR isoforms into secretory vesicles, the nucleus or the soluble phase. OTR could potentially enter the soluble phase following its internalization from the membrane as was shown previously for PTHrP [39].

OT has been shown to have many, sometimes opposite, effects in a variety of cells. Thus, OT may either promote [6, 9, 40, 41] or inhibit cell proliferation [11, 16]. The type of tissue or cell may not be the only factor determining the biological impact of OT. Thus, caveolae-localized OTR has been shown to elicit a potent mitogenic signal without internalization while activation of plasma membrane-localized OTR leads to the OTR internalization and growth inhibition [17,19]. The biological significance of the nuclear localization of GPCRs can be related to the regulation of nuclear events directly in the nucleus and nuclear localization of GPCRs can be necessary for their full transcriptional activity [33, 42]. The functionality of nuclear GPCRs is suggested by their association in the nucleus with G-proteins and enzymatic effectors [43]. In addition, activation of nuclear GPCRs induce enzymatic effects in the nucleus and different cellular effects upon activation of surface and nuclear GPCRs has been described [21]. Since the significance of the localization of OTR in the nucleus is not understood at this time, we can only form a hypothesis concerning the function of the nuclear or putative intracrine OTRs. Recently, OT has been reported to up-regulate the gene expression of different adhesion-related molecules in tumour-derived endothelial cells [41]: the

present evidence suggests that -beside activating the 'classical' intracytoplasmic signaling cascade- OT could be transferred to the cell nucleus and directly activate transcriptional factors promoting the 'switch on' of specific genes. It may be asserted that the very existence of the constitutive and ligand-dependent translocation is perhaps indicative of the functional importance of the OT/OTR system in the nuclei of various type of cells: once again, concerning the OT/OTR system, the 'un-expected is not over' [13], yet.

## Acknowledgements

We thank James Daniero and Dr. Joseph Moore of the Bucknell Imaging Facility for their invaluable help and Karen Shrawder for the help in preparation of the manuscript. This paper was supported by grants from AIRC (Associazione Italiana per la Ricerca sul Cancro), MURST and Compagnia di San Paolo 'Special Project Oncology'.

## References

1. **Bussolati G, Cassoni P, Ghisolfi G, Negro, F, Sapino, A.** Immunolocalization and gene expression of oxytocin receptors in carcinomas and non-neoplastic tissues of the breast. *Am J Pathol.* 1996; 148: 1895–903.
2. **Sheldrick EL, Flick-Smith HC.** Effect of ovarian hormones on oxytocin receptor concentrations in explants of uterus from ovariectomized ewes. *J Reprod Fert.* 1993; 97: 241–5.
3. **Gimpl G, Fahrenholz F.** The oxytocin receptor system: structure, function, and regulation. *Physiol Rev.* 2001; 81: 629–83.
4. **Einspanier A, Ivell R.** Oxytocin and oxytocin receptor expression in reproductive of the male marmoset monkey. *Biol Reprod.* 1997; 56: 416–22.
5. **Cassoni P, Marrocco T, Sapino A, Allia E, Bussolati G.** Evidence of oxytocin/oxytocin receptor interplay in human prostate gland and carcinomas. *Int J Oncol.* 2004; 25: 899–904.
6. **Thibonnier M, Conarty DM, Preston JA, Plesnicher CL, Dweik RA, Erzurum SC.** Human vascular endothelial cells express oxytocin receptors. *Endocrinology.* 1999; 140: 1301–9.
7. **Breton C, Haenggeli C, Barberis C, Heitz F, Bader CR, Bernheim L, Tribollet E.** Presence of functional oxytocin receptors in cultured human myoblasts. *J Clin Endocrinol Metab.* 2002; 87: 1415–8.

8. **Copland JA, Ives KL, Simmons DJ, Soloff MS.** Functional oxytocin receptors discovered in human osteoblasts. *Endocrinology*. 1999; 140: 4371–4.
9. **Cassoni P, Sapino A, Deaglio S, Bussolati B, Volante M, Munaron L, Albini A, Torrisi A, Bussolati G.** Oxytocin is a growth factor for Kaposi's sarcoma cells: evidence of endocrine-immunological cross-talk. *Cancer Res*. 2002; 62: 2406–13.
10. **Pequeux C, Breton C, Hagelstein MT, Geenen V, Legros JJ.** Oxytocin receptor pattern of expression in primary lung cancer and in normal human lung. *Lung Cancer*. 2005; 50: 177–88.
11. **Cassoni P, Sapino A, Stella A, Fortunati N, Bussolati G.** Presence and significance of oxytocin receptors in human neuroblastomas and glial tumors. *Int J Cancer*. 1998; 77: 695–700.
12. **Novak JF, Judkins MB, Chernin MI, Cassoni P, Bussolati G, Nitche JA, Nishimoto SK.** A plasmin-derived hexapeptide from the carboxyl end of osteocalcin counteracts oxytocin-mediated growth inhibition of osteosarcoma cells. *Cancer Res*. 2000; 60: 3470–6.
13. **Bussolati G, Cassoni P.** The oxytocin/oxytocin receptor system – expect the unexpected. *Endocrinology*. 2001; 142: 1377–9.
14. **Flint APF, Leat WM, Sheldrick EL, Stewart HJ.** Stimulation of phosphoinositide hydrolysis by oxytocin and the mechanism by which oxytocin controls prostaglandin synthesis in the ovine endometrium. *Biochem J*. 1986; 237: 797–805.
15. **Anwer K, Hovington JA, Sanborn BM.** Involvement of protein kinase A in the regulation of intracellular free calcium and phosphoinositide turnover in rat myometrium. *Biol Reproduct*. 1990; 43: 851–9.
16. **Cassoni P, Sapino A, Fortunati N, Munaron L, Chini B, Bussolati G.** Oxytocin inhibits the proliferation of MDA-MB231 human breast-cancer cells *via* cAMP and PKA. *Int J Cancer*. 1997; 72: 340–4.
17. **Rimoldi V, Reversi A, Taverna E, Rosa P, Francolini M, Cassoni P, Parenti M, Chini B.** Oxytocin receptor elicits different EGFR/MAPK activation patterns depending on its localization in caveolin-1 enriched domains. *Oncogene*. 2003; 22: 6054–60.
18. **Pequeux C, Keegan BP, Hagelstein MT, Geenen V, Legros JJ, North WG.** Oxytocin- and vasopressin-induced growth of human small-cell lung cancer is mediated by the mitogen-activated protein kinase pathway. *Endocr Relat Cancer*. 2004; 11: 871–85.
19. **Guzzi F, Zanchetta D, Cassoni P, Guzzi V, Francolini M, Parenti M, Chini B.** Localization of the human oxytocin receptor in caveolin-1 enriched domains turns the receptor-mediated inhibition of cell growth into a proliferative response. *Oncogene*. 2002; 21: 1658–67.
20. **Luttrell LM.** Activation and targeting of mitogen-activated protein kinases by G-protein-coupled receptors. *Can J Physiol Pharmacol*. 2002; 80: 375–82.
21. **Gobeil F, Fortier A, Zhu T, Bossolasco M, Leduc M, Grandbois M, Heveker N, Bkaily G, Chemtob S, Barbaz D.** G-protein-coupled receptors signalling at the cell nucleus: an emerging paradigm. *Can J Physiol Pharmacol*. 2006; 84: 287–97.
22. **Re RN, Cook JL.** The intracrine hypothesis: an update. *Regul Pept*. 2006; 133: 1–9.
23. **Kimura T, Tanizawa O, Mori K, Brownstein MJ, Okayma H.** Structure and expression of a human oxytocin receptor. *Nature*. 1992; 356: 526–9.
24. **Kimura T, Takemura M, Nomura S, Nobunaga T, Kubota Y, Inoue T, Hashimoto K, Kumazawa I, Ito Y, Ohashi K, Koyama M, Azuma C, Kitamura Y, Saji F.** Expression of oxytocin receptor in human pregnant myometrium. *Endocrinology*. 1996; 137: 780–5.
25. **Belgrader P, Cheng J, Zhou X, Stephenson LS, Maquat LE.** Mammalian nonsense codons can be cis effectors of nuclear mRNA half-life. *Mol Cell Biol*. 1994; 14: 8219–28.
26. **Phaneuf S, Asboth G, Carrasco MP, Linares BR, Kimura T, Harris A, Bernal AL.** Desensitization of oxytocin receptors in human myometrium. *Human Reprod Update*. 1998; 4: 625–33.
27. **Berrada K, Plesnicher CL, Luo X, Thibonnier M.** Dynamic interaction of human vasopressin/oxytocin receptor subtypes with G protein-coupled receptor kinases and protein kinase C after agonist stimulation. *J Biol Chem*. 2000; 275: 27229–37.
28. **Fricke M, Hollinshead M, White N, Vaux D.** Interphase nuclei of many mammalian cell types contain deep, dynamic, tubular membrane-bound invaginations of the nuclear envelope. *J Cell Biol*. 1997; 136: 531–44.
29. **Grande MA., van der Kraan I, van Steensel B, Schul W, de The H, van der Voort HTM, de Jong L, van Driel R.** PML-containing nuclear bodies: their spatial distribution in relation to other nuclear components. *J Cell Biochem*. 1996; 63: 280–91.
30. **Swindle CS, Tran KT, Johnson TD, Banerjee P, Mayes AM, Griffith L, Wells A.** Epidermal growth factor (EGF)-like repeats of human tenascin-C as ligands for EGF receptor. *J Cell Biol*. 2001; 154: 459–68.
31. **Jans DA, Xiao CY, Lam MHC.** Nuclear targeting signal recognition: a key control point in nuclear transport? *Bio Essays*. 2000; 22: 532–44.
32. **Cullen BR, Hauber J, Campbell K, Sodroski JG, Halesline WA, Rosen CA.** Subcellular location of the human immunodeficiency virus trans-acting art gene product. *J Virol*. 1988; 62: 2498–501.
33. **Thebault S, Basbous J, Gay B, Devaux C, Mesnard JM.** Sequence requirement for the nucleolar localization of human I-mfa domain-containing protein (HIC p40). *Europ J Cell Biol*. 2000; 79: 834–8.
34. **Wells A, Marti U.** Signalling shortcuts: cell-surface receptors in the nucleus? *Nat Rev Mol Cell Biol*. 2002; 3: 697–702.

35. **Bugler B, Amalric F, Prats H.** Alternative initiation of translation determines cytoplasmic or nuclear localization of basic fibroblast growth factor. *Mol Cell Biol.* 1991; 11: 573–7.
36. **Florkiewicz RZ, Baird A, Gonzalez AM.** Multiple forms of bFGF differential nuclear and cell surface localization. *Growth Factors.* 1991; 4: 265–75.
37. **Nguyen MTA, He B, Karaplis AC.** Nuclear forms of parathyroid hormone-related peptide are translated from non-AUG start sites downstream from the initiator methionine. *Endocrinology.* 2001; 142: 694–703.
38. **Rozen F, Russo C, Banville D, Zingg HH.** Structure, characterization, and expression of the rat oxytocin receptor gene. *Proc Natl Acad Sci USA.* 1995; 92: 200–4.
39. **Watson PH, Fraher LJ, Natale BV, Kisiel M, Hendy GN, Hodsman AB.** Nuclear localization of the type 1 parathyroid hormone/parathyroid hormone-related peptide receptor in MC3T3-E1 cells: association with serum-induced cell proliferation. *Bone.* 2000; 26: 221–5.
40. **Cassoni P, Sapino A, Munaron L, Deaglio S, Chini B, Graziani A, Ahmed A, Bussolati G.** Activation of functional oxytocin receptors stimulates cell proliferation in human trophoblast and choriocarcinoma cell lines. *Endocrinology.* 2001; 142: 1130–6.
41. **Cassoni P, Marrocco T, Bussolati B, Allia E, Munaron L, Sapino A, Bussolati G.** Oxytocin induces proliferation and migration in immortalized human dermal microvascular endothelial cells and human breast tumor-derived endothelial cells. *Mol Cancer Res.* 2006; 4: 351–9.
42. **Re R.** The nature of intracrine peptide hormone action. *Hypertension.* 1999; 34: 534–8.
43. **Willard FS, Crouch MF.** Nuclear and cytoskeletal translocation and localization of heterotrimeric G-proteins. *Immunol Cell Biol.* 2000; 78: 387–94.